Environ. Sci. Technol. **2006**, *40,* 2944−2950

Experimentally Altered Groundwater Inflow Remobilizes Acidity from Sediments of an Iron Rich and Acidic Lake

KLAUS-HOLGER KNORR AND
CHRISTIAN BLODAU*

Limnological Research Station and Department of Hydrology, University of Bayreuth, D-95440 Bayreuth, Germany

To study the impact of changes in groundwater flow and chemistry on acidity export from sediments in acid mine drainage (AMD) polluted lakes, a column experiment was carried out. Schwertmannite rich sediment was subjected to three different flow rates (0, 5, and 20 L m^{-2} a^{-1}), two percolate chemistries (1/1 mmol L^{-1} vs 10/15 mmol L^{-1} sulfate/ferrous iron, pH 5), and DOC input (∼2.5 mmol C L^{-1}). Percolation induced acidity export in all percolated treatments (8.8−40.4 mol m^{-2} a^{-1}) by accelerated proton generation from schwertmannite transformation (18.0−35.9 mol m^{-2} a^{-1}) and ferrous iron release (3.8−11.6 mol m^{-2} a^{-1}) from the sediment matrix. Mobilization increased with flow rate and decreased with sulfate and iron concentrations. Unspecifically bound ferrous iron contents increased within the sediment (up to 40.5 mol m^{-2} a^{-1}) when iron concentrations in the percolate were high. Reduced sulfur species formed following raises in pH, but acidity consumption through this process (0.3−6.6 mol m^{-2} a^{-1}) and the formation of carbonates (0.11−0.45 mol m^{-2} a^{-1}) remained small. The study thus suggests that increases in groundwater inflow remobilize acidity from AMD polluted sediments.

Introduction

A growing number of mine pit lakes in Europe and North America is strongly acidified by acid mine drainage (AMD) (*1*, *2*). A primary mechanism of acidification is the precipitation of ferric iron, following the input of anoxic groundwater enriched in ferrous iron (*3*, *4*). Input of protons often plays a lesser role for acidification, as the groundwaters are typically buffered by calcite and silicate weathering in the aquifers and are often only weakly acidic (*3*, *4*). The acidification of the surface waters might in part be reversed by microbial reduction of SO_4^{2-}, NO_3^-, Fe, Mn, and the production of NH_4^+ in sediments (*5*). If the reduced products are sequestered, e.g. in the form of iron sulfides, alkalinity is permanently gained (*6*). In strongly AMD polluted lakes, however, sediments may also release protons owing to precipitation of the iron mineral schwertmannite ($FeO(OH)_x(SO_4)_y$, $1 - x = 0.25y$, $0.125 < y < 0.22$) and its subsequent transformation to goethite (*7*, *8*). The occurrence of this process has been confirmed for a wide range of AMD polluted surface waters (*9*, *10*). Factors that control the net balance of acidity consumption and generation in the sediments are thus of considerable interest.

Previous investigations documented that acidity consumption and generation are directly controlled by the sediment pore water pH (*11*, *12*). Values of pH 5 and higher not only were required for the formation of iron sulfides and carbonates (*3*, *11*) but also accelerated the transformation of schwertmannite in batch experiments (*10*). It was further documented that sediment pH can be elevated in lake areas with sustained groundwater inflow (*4*). As a consequence, iron sulfide and carbonate formation rates increased, and the acidity balance of the sediments was modified (*4*, *8*, *13*, *14*). However, we are lacking information regarding the impact of increasing groundwater flow on the acidity balance of sediments previously unaffected by percolation. In particular there is concern that increasing groundwater inflow will release stored acidity by remobilization of ferrous iron and accelerated transformation of schwertmannite. Increases in groundwater flow with time are a widespread consequence of water management measures in landscapes affected by mining (*15*) and may also occur in soft water lakes on a seasonal basis (*7*, *8*, *16*). To elucidate this critical issue, we quantified acidity generation and consumption for sediments relative to a control in column experiments. Flow rates and chemistry were varied within a range typically encountered in strongly AMD polluted lakes.

Materials and Methods

Lake 77 in Lusatia, Germany, contains schwertmannite and goethite rich sediments and has previously served as a model system with respect to iron and sulfur cycling (e.g. refs *4*, *17*, and *13*). It is acidic (pH 2.8), 8 m deep with an area of 24.4 ha, and chemically dominated by sulfate (8−13 mmol L^{-1}), ferric iron (0.8 to 2 mmol L^{-1}), and ferrous iron (20 μmol L^{-1} to 6 mmol L^{-1}). Anoxic conditions develop in the hypolimnion. Groundwater inflow increases from about 1.5 L m^{-2} d^{-1} in the center to >10 L m^{-2} d^{-1} near the shores (*18*). These values are similar as in other acidic mine and soft water lakes (*3*, *14*, *15*, *19*). Groundwater entering from dump aquifers had a pH of 3.4−5.2 and contained 5−60 mmol L^{-1} sulfate and 5−20 mmol L^{-1} ferrous iron (*4*).

The experiment was set up in a constant temperature chamber by filling airtight Plexiglas columns (inner diameter 8 cm, length 25 cm) with homogenized sediment layers under an argon stream up to a height of 15 cm. The original sediment and redox layering was preserved. Ten cm of deaerated lake water were added on top. Sixteen gravity cores (∅ 6 cm) were sampled from the center of the lake (inflow <2 L m^{-2} d^{-1}) in January 2004. Visually similar layers of these cores were pooled and homogenized under an inert gas atmosphere. Sediment color changed from bright orange at the surface to dark gray brown at a depth of 12−15 cm. Values of pore water pH increased from 2.5 to 3.1 in the upper 6 cm to 5.4 at a depth of 12−15 cm. Organic carbon contents ranged from 4.5 to 10.3%, and total iron contents decreased from 400 to 425 mg g^{-1} dw in the upper 6 cm to 14 mg g^{-1} dw at a depth of 12−15 cm.

Four columns were upward-percolated at two flow rates with solution representing either AMD polluted (dump) or pristine (background) groundwater (Table 1), resembling conditions in the watershed of Lake 77. Two unpercolated columns (C1, C2) served as controls. C1 was sampled after 10 days to determine initial conditions and C2 after 95 days for comparison with the percolated treatment. The percolates also contained Ca^{2+} (5 mM), K^+ (1 mM), Mg^{2+} (2 mM), NH_4^+ (0.3 mM), Al^{3+} (0.1 mM), Na^+ (20 mM), Fe^{3+} (0.1−0.5 mM), Cl^- (18 mM or 30 mM), and Br^- (1 mM) as a tracer. Percolates were adjusted to pH 5 using HCl or NaOH and kept in 5 L glass bottles under a nitrogen atmosphere. The columns were incubated at 10 °C for the first 69 days and at 20 °C thereafter.

---

* Corresponding author phone: 49 921 552223; fax: 49 921 552366; e-mail: christian.blodau@uni-bayreuth.de.

10.1021/es051874u CCC: $33.50

TABLE 1. Description of Treatments and Contribution of Reactive Iron to the Total Iron Content (A) and TRIS Content (B) in the Treatments versus Depth[a,b]

treatment	C1	C2	BL	BH	DL	DH
solution	control	control	background (pH 5)[c]		dump (pH 5)[d]	
inflow (mm d^{-1})			~5	~20	~5	~20
(L m^{-2} d^{-1})			5.9 ± 1.6	20.6 ± 2.0	5.9 ± 1.6	20.6 ± 2.0
depth (cm)	**C1**	**C2**	**BL**	**BH**	**DL**	**DH**
			A: Contribution of Reactive Iron to Total Iron (%), Reactive Ferrous Iron in Parentheses (%)			
−0.4	101.1 (3.9)	75.6 (4.5)	76.5 (3.3)	44.4 (2.5)	44.5 (4.6)	54.4 (4.7)
−1.4	91.1 (3.1)	60.2 (3.8)	56.0 (2.2)	30.3 (1.4)	37.8 (2.5)	30.1 (3.0)
−3.0	68.5 (2.9)	37.2 (4.5)	29.9 (2.9)	19.4 (2.3)	35.4 (4.3)	21.2 (4.1)
−5.0	31.7 (3.0)	23.2 (6.0)	23.3 (3.2)	16.4 (3.8)	28.5 (7.8)	18.2 (4.8)
−7.0	28.1 (3.9)	23.3 (7.5)	18.3 (5.9)	27.8 (9.6)	23.4 (7.8)	22.7 (6.3)
−10.0	37.0 (12.7)	31.2 (15.5)	29.8 (11.3)	29.7 (14.5)	36.2 (17.1)	30.8 (14.6)
−13.5	36.2 (16.1)	27.3 (17.0)	27.4 (15.5)	39.2 (21.7)	49.0 (29.5)	31.4 (16.7)
			B: TRIS Content (μmol g^{-1}), AVS Content in Parentheses (μmol g^{-1}, "-" if <0.1)			
−0.4	1.8 (0.1)	2.9 (0.1)	1.1 (−)	7.6 (−)	2.9 (−)	8.9 (−)
−1.4	2.1 (−)	2.2 (−)	2.3 (−)	3.9 (−)	2.4 (−)	4.2 (−)
−3.0	3.0 (−)	2.8 (−)	2.6 (0.4)	3.2 (0.1)	2.9 (0.1)	4.6 (0.1)
−5.0	5.5 (0.1)	4.2 (−)	3.3 (0.1)	9.4 (0.1)	5.3 (0.1)	5.4 (0.1)
−7.0	10.2 (0.1)	16.2 (0.1)	9.4 (−)	28.6 (0.1)	12.8 (−)	15.0 (0.3)
−10.0	65.3 (0.1	70.1 (0.1)	54.6 (−)	77.5 (0.1)	58.5 (0.3)	64.6 (0.2)
−13.5	102.8 (0.2)	118.6 (0.1)	127.4 (−)	119.5 (0.4)	141.5 (0.3)	98.8 (−)

[a] Control C1 was sampled after 10 days, all other treatments after 95 days. [b] Column labels: first letter B: background iron and sulfate concentrations in the percolate, D: dump treatments percolated with groundwater rich in ferrous iron and sulfate; second letter: L: low groundwater inflow, H: high groundwater inflow. [c] 1 mmol L^{-1} Fe^{2+} and 1 mmol L^{-1} SO_4^{2-}. [d] 15 mmol L^{-1} Fe^{2+} and 10 mmol L^{-1} SO_4^{2-}.

As an additional carbon source, we added a leaf litter extract (~2.5 mmol C L^{-1}) after day 46 (Supporting Information, section C). The overlying anoxic water phase, representing summer conditions, was sampled through a gastight septum. Permanently installed electrodes were used to measure pH and pH_2S.

The experiment was terminated by cutting the cores into segments of 0−0.8 cm, 0.8−2 cm, 2−4 cm, 4−6 cm, 6−8 cm, 8−12 cm, and 12−15 cm. Bulk density ranged from 0.055 g cm^{-3} (±0.007) at the top to 0.452 g cm^{-3} (±0.039) at the bottom. Pore water was obtained by centrifugation and analyzed for Fe^{2+}, Fe^{3+}, Ca^{2+}, Al^{3+}, NH_4^+, SO_4^{2-}, Cl^-, and Br^-. The solid sediment was kept at −25° C until analyzed. Additional information regarding the site and setup are provided in the Supporting Information.

Liquid- and Solid-Phase Analyses. Anions were determined using ion chromatography (Metrohm IC-system, METROSEP Anion Dual 1 column, chemical suppression). Total dissolved iron was measured by flame atomic absorption spectroscopy (AAS, Varian SpectrAA-20). Fe^{2+} was determined by the phenanthroline method (*20*). Ferric iron concentration was calculated as $[Fe^{3+}] = [Fe(tot)] - [Fe^{2+}]$. Total solid phase sulfur was determined in freeze-dried samples using a CNS-analyzer (Vario EL, Germany). The content of total reduced inorganic sulfur (TRIS: FeS_2, FeS, S°) and acid volatile sulfur (AVS: FeS) was quantified according to ref *21*. Total iron was determined by AAS after digestion of dried sediment with concentrated nitric and hydrochloric acid (1:1 ratio). Reactive iron and carbonates were extracted with 1 N HCl (*22*) in gastight septum bottles. CO_2 was measured in the headspace by gas chromatography (HP 6890 GC/TCD). The mineralogical composition was analyzed by Fourier transformed infrared spectroscopy (Supporting Information).

Acidity Budgets. Acidity was redefined for a heterogeneous, iron-rich system with HCO_3^-, H_2O, NH_4^+, HS^-, and SO_4^{2-} as dissolved and $FeO(OH)_{0.575}(SO_4)_{0.2125}$ and $Al(OH)_3$ as solid-phase reference species. We assumed that at the equivalence point of HCO_3^-, dissolved aluminum and ferric iron species would precipitate and release protons. As the reference space of interest is the oxic lake compartment, ferrous iron was assumed to be oxidized and precipitated as schwertmannite ($FeO(OH)_{0.575}(SO_4)_{0.2125}$). These considerations are in agreement with the following definition (eq 1):

$$\begin{aligned} Ac_{(HCO_3^-)} = {} & 1.575[Fe^{2+}] + 2.575[Fe^{3+}] + \\ & 1.575[Fe(OH)^{2+}] + 0.575[Fe(OH)_2^{+}] + 3[Al^{3+}] + \\ & 2[Al(OH)^{2+}] + [Al(OH)_2^{+}] + [H_2S] + [H^+] + [HSO_4^-] + \\ & [H_2CO_3] - [S^{2-}] - [NH_3] - [OH^-] - 0.425[Fe(OH)_{3,aq}] - \\ & 1.425[Fe(OH)_4^-] - [Al(OH)_4^-] \quad (1) \end{aligned}$$

Acidity fluxes from the sediment columns were calculated using the in- and output of acidity and using eq 1 (based on the schwertmannite stoichiometry determined in ref *17*). Speciation was calculated using the PHREEQC algorithm version 2.8.02 and thermodynamic database (*23*). The contribution of aluminum and sulfur species, NH_3, and OH^- to acidity fluxes was calculated and found to be <2% altogether; hence, it was not further considered. Some acidity sources and sinks were estimated relative to control treatment C1 using eqs 2−6, representing the generation of protons by schwertmannite transformation (*2*), the consumption of protons by FeS_2 and FeS formation in the sediment (*3*, *4*), and the generation of protons after export and oxidation of ferrous iron in the lake compartment (*5*). We assumed TRIS to be mainly FeS_2, as had previously been determined (*4*, *13*)

$$0.425H_2O + FeO(OH)_{0.575}(SO_4)_{0.2125} \Rightarrow FeOOH + 0.2125SO_4^{2-} + 0.425H^+ \quad (2)$$

$$3.75{<}CH_2O{>} + FeOOH + 2SO_4^{2-} + 4H^+ \Rightarrow FeS_2 + 3.75CO_2 + 6.25H_2O \quad (3)$$

$$2.25{<}CH_2O{>} + FeOOH + SO_4^{2-} + 2H^+ \Rightarrow FeS + 2.25CO_2 + 3.75H_2O \quad (4)$$

$$Fe^{2+} + 0.25O_2 + 0.2125SO_4^{2-} + 1.075H_2O \Rightarrow FeO(OH)_{0.575}(SO_4)_{0.2125} + 1.575H^+ \quad (5)$$

$$R(\mathrm{Ac}) = \frac{\sum_{i=1}^{n} \Delta[\mathrm{BD}_i \circ z(\mathrm{H}^+) \circ (\mathrm{X}_i)]}{t} \qquad (6)$$

with the following: R(Ac), rate of acidity generation (mol m^{-2} a^{-1}); $\sum_{i=1}^{n}$ sum over layer i to layer n; Δ = difference between treatment and initial composition in control C1 of layer i; BD_i = bulk density (g m^{-3}) of layer i; t = time of incubation (a); $z(H^+)$ stoichiometric factor of H^+ in eqs 2−5; (X_i) = content of solid-phase X in layer i (mol g^{-1}).

Processes that avoid generation of acidity in the lake compartment (eq 5) were assigned to be a proton sink ($z(H^+)$: negative sign), whereas ferrous iron release into the sediment pore water was assumed a proton source ($z(H^+)$: positive sign). Absolute changes in iron solid-phase contents were small compared to total iron contents. Relative changes of the different pools were thus calculated and based on the mean iron content of all treatments. Schwertmannite transformation rates were determined from changes in crystalline iron contents. Net turnover in the columns was calculated from vertical advective-diffusive mass balances using concentration profiles and temperature-corrected diffusion coefficients. Additional information is provided in the Supporting Information.

Results

Column Output. The chemical composition of the effluent differed among the treatments and compared to the control. The bromide tracer breakthrough was accelerated in the high inflow treatments (BH "background high flow", DH "dump high flow"), suggesting some preferential flow, presumably at the wall of the columns (Figure 1 F). The pH in the effluent increased from below 3 to 3.7 (low inflow) and to 4.7−5 (high inflow) by the end of the incubation (Figure 1A). In the background treatments, sulfate concentrations (Figure 1B) increased on average by 6.2 mmol L^{-1} (BL, "background low flow") and 2.8 mmol L^{-1} (BH). Ferrous iron concentrations increased by 8.3 mmol L^{-1} (BL) and 3.3 mmol L^{-1} (BH) (Figure 1 C).

In the dump treatments DL ("dump low flow") and DH, concentration changes were smaller. Ferrous iron concentrations hardly changed along the flow path (~14 − 15 mmol L^{-1}), and sulfate concentrations only slightly increased (12−13 mmol L^{-1} vs 10 mmol L^{-1}). H_2S (max. 26 μmol L^{-1}) was detected in the outflow of the treatments BH, DH, and DL after 60−80 days, indicating sulfate reduction. DOC was initially released, followed by a second output-pulse after addition of DOC to the input (Figure 1E). More than half of the added DOC was either retained or mineralized. DIC concentrations (Figure 1D) followed DOC concentrations with a short time lag.

Pore Water. The pore water had been exchanged by the end of the experiment. This was indicated by chloride concentrations of ~19 (background treatments) and ~30 mmol L^{-1} (dump treatments). In the background treatments, the sulfate concentration was, accordingly, also lowered to a maximum of 6.3 mM (BL) and 2.6 mM (BH). Fe^{2+} concentrations decreased to 8.6 mmol L^{-1} and 4.2 mmol L^{-1}. In the treatments percolated with the dump solution, the sulfate concentration adjusted to a maximum of 16.6 mmol L^{-1} (DL) and 14.8 mmol L^{-1} (DH). Fe^{2+} concentrations slightly increased to 16.9 mmol L^{-1} and 15.8 mmol L^{-1}. Ferric iron concentrations remained small in comparison.

The pore water pH ranged from 3 to 6 and decreased in the order BH ≈ DH > DL > BL ≈ C2 > C1 (Figure 2). A maximum of sulfate and ferrous iron concentrations generally occurred at a depth of ~1.4 cm, indicating schwertmannite transformation and iron reduction close to the sediment surface.

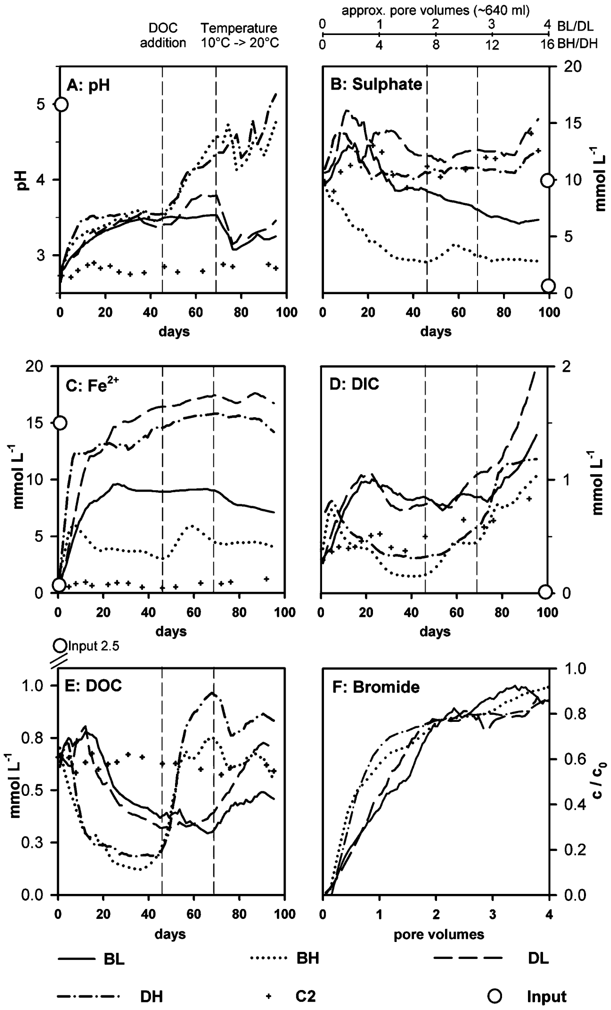

FIGURE 1. Chemical composition of the column output. Changes in experimental conditions are marked with dashed lines, input concentrations with open circles. For bromide (F) the time scale is given in pore volumes (see (B) for comparison). In control C2, conditions remained fairly constant over time in comparison.

Solid-Phase Iron. In the uppermost layer of the control C1, reactive ferric iron consisted mostly of schwertmannite, as indicated by the characteristic FTIR-bands at 1132 cm^{-1} (ν_3-sulfate), 704 cm^{-1} (ν Fe−O), and 614 cm^{-1} (ν_4-sulfate) and by Fe/S ratios of 5.4−6.3 (Figure 3). The schwertmannite content decreased with depth. Percolation also lowered the reactive iron (schwertmannite) contents, relative to the control C1, particularly in the upper 6 cm of sediment (Table 1A, Figure 3). In the treatments with high percolation rates, reactive iron contents decreased most, from ~100% of total iron to 45−55% in the upper layer and from 90 to 32% to 30−16% beneath. In the BL treatment, reactive iron contents decreased the least and remained on a similar level as in the control C2. The small schwertmannite transformation rate in BL coincided with the lowest pH of all percolated treatments (Figure 2). The data were in agreement with the results using FTIR spectroscopy and Fe/S ratios (see section D, Supporting Information). Schwertmannite transformation rates overall increased in the order C1 < C2 < BL < DL ≅ DH < BH.

Reactive ferrous iron contents increased in all treatments, compared to the control C1 by 19−62%, during the incubation, with the exception of BL. Iron sulfides were primarily formed in the BH, DH, and DL treatments, in which H_2S was also detected in the outflow. Absolute TRIS contents were low, reaching concentrations of 0.7−9.4 μmol g^{-1} dw in the

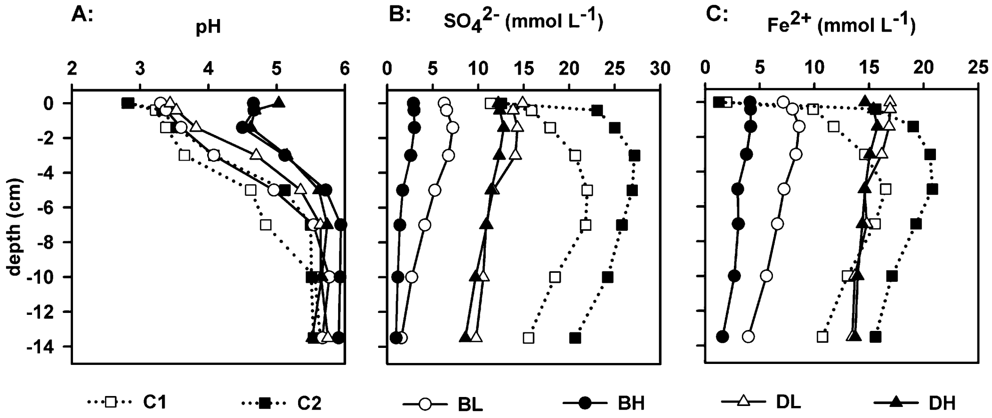

FIGURE 2. Pore water profiles in (A) pH, (B) sulfate, and (C) ferrous iron. Data points represent the mean of at least 3 measurements of the individual sample.

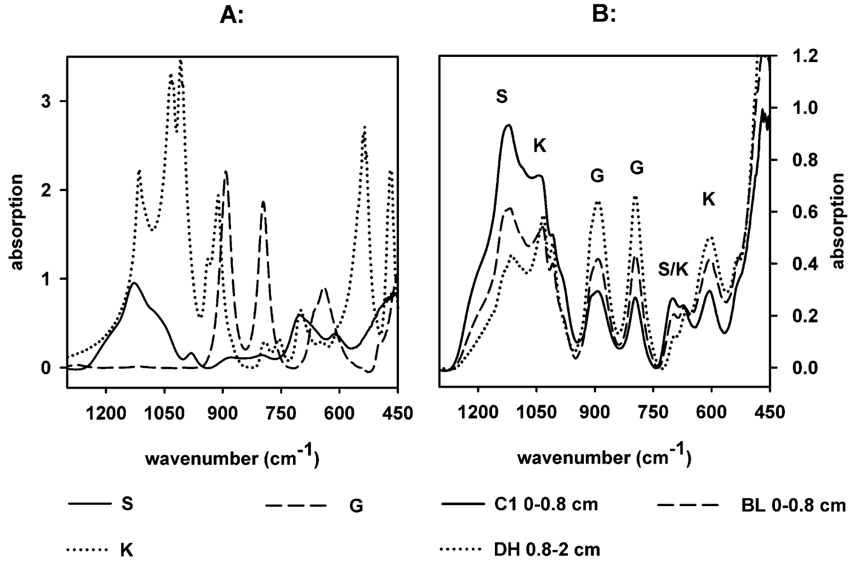

FIGURE 3. FTIR-spectra of pure minerals (A) and selected samples showing increasing transformation from C1 to DH (B). Spectra are means of 30 scans with a resolution of 2 cm^{-1}.

upper 5 cm (Table 1B). The contribution of AVS to TRIS was in most cases negligible (Table 1B in parentheses).

Acidity Flux from the Sediment. Acidity was exported in all treatments (Figure 4, Table 2). In the low inflow treatments, little acidity was released in the first 16 days (17.6 mol m^{-2} a^{-1}, BL) or even consumed (−5.7 mol m^{-2} a^{-1}, DL), as the iron-poor water above the sediment was eluted first. Elution of pore water rich in ferrous iron and acidity followed. Subsequently, acidity was released more constantly (31.2−21.8 mol m^{-2} a^{-1} for BL, 13.2−17.7 mol m^{-2} a^{-1} for DL). In the high inflow treatments, acidity was flushed out within the first 16 days and constantly released thereafter until day 46 (BH: 23.8 mol m^{-2} a^{-1}, DH: 18.1 mol m^{-2} a^{-1}). After the addition of DOC, acidity was strongly released in BH (53.8−50.9 mol m^{-2} a^{-1}) due to accelerating production of ferrous iron and less strongly in DH (17.3−20.4 mol m^{-2} a^{-1}).

As expected, the total acidity efflux was highest in the dump treatments (60.5−190.9 mol m^{-2} a^{-1}). The contribution of the sediments to the acidity efflux, however, was higher in background treatments (66−82% vs 9−15%). More ferrous iron was released from the sediment matrix when iron and sulfate concentrations in the percolate were low. TRIS formation and retention of iron as carbonates consumed only little of the overall acidity flux. Unspecific retention of ferrous iron played a more important role.

Discussion

Iron and Sulfur Transformations. The release of protons, iron, and sulfate from the sediment was in agreement with the transformation of schwertmannite to goethite (Table 1A, Figure 3) and the reductive dissolution of ferric (hydr)oxides. Percolation adjusted the pore water chemistry to the chemistry of the inflowing water. It also raised the pH in the pore water pH, initially because the original pore water was displaced by percolate, later because the addition of electron donors increased iron and sulfate reduction rates (Figure 1). The pH increase in the percolated treatments accelerated the transformation of schwertmannite into goethite (Table 2), as transformation rates increase outside the stability field of the mineral (*9*, *10*). Accordingly, schwertmannite transformation rates were highest in the high inflow treatments BH and DH, in which effluent pH reached 4.7−5 by the end of the experiment.

TRIS was formed in the surface layers of treatments that had reached an average pH value of 4.5−5 and produced H_2S by the end of the experiment (Table 1B and Figure 2). These values are in reasonable agreement with a pH threshold of 4.9 for the initiation of sulfate reduction, as previously determined by Küsel et al. (*24*). However, TRIS contents in the uppermost sediment layers (0.9−9.4 μmol g^{-1} dw) remained small, especially if compared to less iron rich and

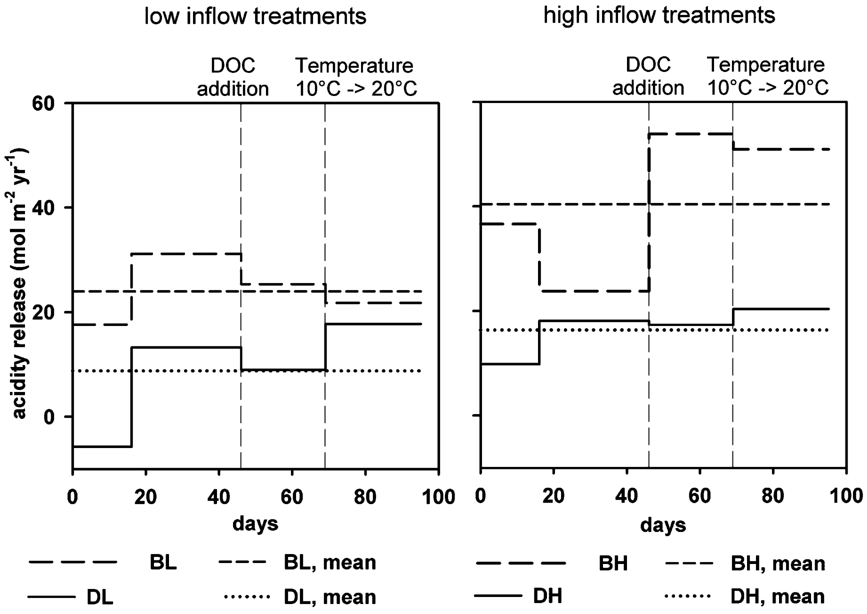

FIGURE 4. Net acidity flux from the sediments. Low inflow treatments are shown on the left, high inflow treatments on the right. The addition of a carbon source (day 46) and the increase in temperature (day 69) are marked by dashed lines.

TABLE 2. Calculated Acidity Fluxes for Lake Water, Sediment Column, and Pore Water Relative to Initial Column C1[a,b]

	acidity fluxes in the treatments ($mol\ m^{-2}\ a^{-1}$)					acidity fluxes in situ ($mol\ m^{-2}\ a^{-1}$)	
process	C2	BL	BH	DL	DH	inflow $< 2\ L\ m^{-2}\ d^{-1}$	inflow $> 10\ L\ m^{-2}\ d^{-1}$
schwertmannite deposition						9.4	9.2
overall acidity input into the lake	0	29.1	61.3	60.5	190.9	1.3	27.4
acidity release from the sediment	0	24.0	40.4	8.8	16.3		
transformation of schwertmannite in the sediment	25.5	31.0	33.6	18.0	35.9	2.4	0.11
TRIS formation in the sediment	−5.1	−0.3	−6.6	−2.1	−2.8	−0.017	−0.12
unspecific retention of Fe(II) in the sediment	−19.4	1.0	−19.1	−40.5	−12.6	−0.08	−0.39
retention/formation of $FeCO_3$ in the sediment	−0.38	0.36	−0.11	−0.14	−0.45	−0.02	−0.14
Fe(II) release (turnover rates from pore water concentration profiles)[d]	4.8	4.0	11.6	3.8	8.0	4.6[c]	3.6[c]

[a] In situ values were taken from ref *4*. Positive values indicate an acidity export from the sediment into the lake water compartment. [b] Positive values indicate a net acidity input into a hypothetical lake water compartment; negative values indicate retention of acidity within the sediment. [c] Calculated from incubation experiments according to data reported in ref *4*. [d] Depth profiles of production rates are provided in the Supporting Information (section E).

pH-neutral sediments in other acidic mine lakes (up to 2100 μmol g^{-1} dw (*11*)) and in soft water lakes (up to 200 μmol g^{-1} dw (*6*)). Even when TRIS formation in the lower sediment layers was included, the contribution of this process to the acidity budget was low (Table 2). Acidity consumption by the formation of carbonates was small in this experiment since the bulk sediment remained undersaturated with respect to siderite. Most of the ferrous iron in the sediments was bound unspecifically, as previously reported (*4*). We assume that ferrous iron was adsorbed on iron oxides in lower sediment layers (*25*), but the obtained data do not allow to clarify this point.

Part of the observed change in process rates was probably driven by the DOC that was added to the percolate. DOC concentrations decreased by ~1.6 mmol L^{-1} along the flowpath, and DIC concentrations were elevated by ~1 mmol L^{-1} in the output. DOC was, therefore, utilized by microbial processes in the sediments, similarly as reported by Frömmichen et al. (*12*). The authors observed that the addition of easily degradable organic matter enhanced iron and sulfate reduction in acidic and iron rich sediments.

Mobilization of Acidity. Lake sediments have been perceived as sinks for acidity in acidified soft water (*5*) and mining lakes (*12*), particularly owing to the formation and burial of iron sulfides (*6*). More recently have sediments been recognized as sources of acidity to water bodies. Acidity is, for example, generated if lake water levels drop, and iron sulfides in littoral sediments are reoxidized (*7*), and if schwertmannite is transformed to goethite in strongly acidified and iron rich systems (*17*, *10*).

This study demonstrates that increases in inflow of groundwater may remobilize acidity from previously unpercolated sediments, even at small flow rates of 5 L m^{-2} d^{-1} (Figure 4, Table 2). A mobilization occurred compared to the unpercolated control and to sustained in situ acidity fluxes (Table 2). It is also in agreement with field data from Lake 77. Total iron contents were lower by 40−60% in sediments receiving sustained groundwater inflow, compared to nonpercolated sediments, despite similar iron sedimentation rates throughout the lake (*4*). Increasing the flow rate by a factor of 4 further enhanced the acidity export by a factor of 1.8. Lowering iron and sulfate concentrations from 10 to 15 mmol L^{-1} to 1 mmol L^{-1} increased the export by a factor of 2.6. Increases in flow rate, DOC concentration, and lower iron and sulfate concentrations in the percolate would thus likely exacerbate a mobilization (Figure 3, Table 2). A considerable fraction of ferrous iron provided with the percolate or reductively dissolved was, however, also retained by mechanisms that were not investigated (Table 2). These mechanisms and the chemical controls involved deserve further attention.

In comparison to the field studies of Peine et al. and Blodau (*4*, *13*, *17*), acidity fluxes, sources, and sinks were much larger in this experimental study (Table 2). Caution is thus appropriate regarding the extrapolation of the determined rates to AMD polluted lakes. Such differences are commonly observed between data stemming from batch, column, and field approaches (*26*). In this case, the differences were probably caused by the addition of DOC, i.e., electron donors and the physical disturbance of the sediment microstructure.

Despite the limitations of the approach, the suggested remobilization of acidity seems a realistic scenario for many AMD polluted lakes. A fairly wide range of percolate chemistries and flow rates was used and provided consistent results in the experiments. Schwertmannite rich sediments are furthermore characteristic for such waters, as has been shown for AMD polluted surface waters in the United States and Korea (*9*, *27*), acid mine drainage treatment ponds (*28*), and recently also for 18 acidic mine lakes (*10*). In even more acidic sediments, increases in pore water pH also lead to transformation of jarosite and acidity release (*29*). Seepage of groundwater into surface waters frequently occurs, particularly along lakeshores (*3*, *13*, *14*, *18*). Advective flow rates ranged from -14.6 to $14.7\ \mathrm{L\ m^{-2}\ d^{-1}}$ in reported studies, which is a similar range as used in our experiments. Temporal variations of flow rates occur in lakes across seasons and years (*16*, *19*), particularly in regions affected by surface mining. Groundwater flow patterns in these regions may even be reversed with changes in mining operations and groundwater management (*17*). Finally, it has to be considered that the potential for iron sulfide formation is limited in these waters because electron donors are in short supply. The productivity of acidic mine lakes is low (*30*, *31*), and the organic matter was found to be fairly recalcitrant and was stabilized by adsorption on iron oxides (*32*). A mechanism that could effectively impede the export of acidity will thus be lacking in many lakes when increases in groundwater inflow occur.

Acknowledgments

We thank K. Söllner and S. Hammer for technical assistance and Drs. K. Küsel, S. Peiffer, J. Breu, and C. McCammon for valuable discussions. K-H. Knorr was supported by a fellowship of the German National Academic Foundation.

Supporting Information Available

A map of Lake 77, groundwater and sediment data, a diagram of the experimental setup, details on DOC preparation, solid-phase characteristics, and turnover rates. This material is available free of charge via the Internet at http://pubs.acs.org.

Literature Cited

(1) Schnoor, J. L.; Galloway, J. N.; Moldan, B. East Central Europe: An environment in transition. *Environ. Sci. Technol.* **1997**, *31*, 412A−416A.

(2) Miller, G. C.; Lyons, W. B.; Davis, A. Understanding the water quality of pit lakes. *Environ. Sci. Technol.* **1996**, *30*, A118−A123.

(3) Bozau, E.; Strauch, G. Hydrogeological basis for biotechnological remediation of the acidic mining lake 'RL 111', Lusatia (Germany). *Water, Air, Soil Pollut.: Focus* **2002**, *2*, 15−25.

(4) Blodau, C. Evidence for a hydrologically controlled iron cycle in acidic and iron rich sediments. *Aquat. Sci.* **2004**, *66*, 47−59.

(5) Schiff, S. L.; Anderson, R. F. Alkalinity Production in Epilimnetic Sediments − Acidic and Nonacidic Lakes. *Water, Air, Soil Pollut.* **1986**, *31*, 941−948.

(6) Giblin, A. E.; Likens, G. E.; White, D.; Howarth, R. W. Sulfur Storage and Alkalinity Generation in New-England Lake-Sediments. *Limnol. Oceanogr.* **1990**, *35*, 852−869.

(7) Yan, N. D.; Keller, W.; Scully, N. M.; Lean, D. R. S.; Dillon, P. J. Increased UV-B penetration in a lake owing to drought-induced acidification. *Nature* **1996**, *381*, 141−143.

(8) Schafran, G. C.; Driscoll, C. T. Porewater Acid-Base Chemistry in near-Shore Regions of an Acidic Lake - the Influence of Groundwater Inputs. *Biogeochemistry* **1990**, *11*, 131−150.

(9) Bigham, J. M.; Schwertmann, U.; Traina, S. J.; Winland, R. L.; Wolf, M. Schwertmannite and the chemical modelling of iron in acid sulfate waters. *Geochim. Cosmochim. Acta* **1996**, *60*, 2111−2121.

(10) Regenspurg, S.; Brand, A.; Peiffer, S. Formation and stability of schwertmannite in acidic mining lakes. *Geochim. Cosmochim. Acta* **2004**, *68*, 1185−1197.

(11) Blodau, C.; Peiffer, S. Thermodynamics and organic matter: constraints on neutralization processes in sediments of highly acidic waters. *Appl. Geochem.* **2003**, *18*, 25−36.

(12) Froemmichen, R.; Wendt-Potthoff, K.; Friese, K.; Fischer, R. Microcosm Studies for Neutralization of Hypolimnic Acid Mine Pit Lake Water (pH 2.6). *Environ. Sci. Technol.* **2004**, *38*, 1877−1887.

(13) Blodau, C. Groundwater inflow controls acidity fluxes in an iron rich and acidic lake. *Acta Hydrochim. Hydrobiol.* **2005**, *33*, 104−117.

(14) Sebestyen, S. D.; Schneider, R. L. Seepage patterns, pore water, and aquatic plants: hydrological and biogeochemical relationship in lakes. *Biogeochemistry* **2004**, *68*, 383−409.

(15) Werner, F.; Bilek, F.; Luckner, L. Impact of regional groundwater flow on the water quality of an old post mining lake. *Ecol. Eng.* **2001**, *17*, 133−142.

(16) Schafran, G. C.; Driscoll, C. T. Flow Path Composition Relationships for Groundwater Entering an Acidic Lake. *Water Resour. Res.* **1993**, *29*, 145−154.

(17) Peine, A.; Tritschler, A.; Kusel, K.; Peiffer, S. Electron flow in an iron-rich acidic sediment - evidence for an acidity-driven iron cycle. *Limnol. Oceanogr.* **2000**, *45*, 1077−1087.

(18) Knoll, D.; Weber, L.; Schafer, W. Groundwater influx to old residual lakes in the brown coal open-pit mining area of Niederlausitz, Germany. *Grundwasser* **1999**, *4*, 55−61.

(19) Kishel, H. F.; Gerla, P. J. Characteristics of preferential flow and groundwater discharge to Shingobee Lake, Minnesota, USA. *Hydrol. Process.* **2002**, *16*, 1921−1934.

(20) Tamura, H.; Goto, K.; Yotsuyanagi, T.; Nagayama, M. Spectrophotometric determination of iron(II) with 1,10-phenanthroline in the presence of large amounts of iron(III). *Talanta* **1974**, *21*, 314−318.

(21) Fossing, H.; Joergensen, B. B. Measurement of bacterial sulphate reduction in sediments: Evaluation of a single step chromium reduction method. *Biogeochemistry* **1989**, *8*, 205−222.

(22) Wallmann, K.; Hennies, K.; König, K. I.; Petersen, W.; Knauth, H. D. New procedure for determining reactive Fe(III) and Fe(II) minerals in sediments. *Limnol. Oceanogr.* **1993**, *38*, 1803−1812.

(23) Parkhurst, D. L. User's guide to PHREEQC- -A computer program for speciation, reaction-path, advective-transport, and inverse geochemical calculations. *Water-Resour. Invest. Rep. (U. S. Geol. Surv.)* **1995**, *95*, 4227−4370.

(24) Küsel, K.; Roth, U.; Trinkwalter, T.; Peiffer, S. Effect of pH on the anaerobic microbial cycling of sulfur in mining-impacted freshwater lake sediments. *Environ. Exp. Bot.* **2001**, *46*, 213−223.

(25) Urrutia, M. M.; Roden, E. E.; Fredrickson, J. K.; Zachara, J. M. Microbial and surface chemistry controls on reduction of synthetic Fe(III) oxide minerals by the dissimilatory iron-reducing bacterium Shewanella alga. *Geomicrobiol. J.* **1998**, *15*, 269−291.

(26) Malmstrom, M. E.; Destouni, G.; Banwart, S. A.; Stromberg, B. H. E. Resolving the scale-dependence of mineral weathering rates. *Environ. Sci. Technol.* **2000**, *34*, 1375−1378.

(27) Yu, J.-Y.; Heo, B.; Choi, I.-K.; Cho, J.-P.; Chang, H.-W. Apparent solubilities of schwertmannite and ferrihydrite in natural stream waters polluted by mine drainage. *Geochim. Cosmochim. Acta* **1999**, *63*, 3407−3416.

(28) Gagliano, W. B.; Brill, M. R.; Bigham, J. M.; Jones, F. S.; Traina, S. J. Chemistry and mineralogy of ochreous sediments in a constructed mine drainage wetland. *Geochim. Cosmochim. Acta* **2004**, *68*, 2119−2128.

(29) Herzsprung, P.; Friese K.; Frömmichen, R.; Göttlicher, J.; Koschorreck, M.; v. Tümpling, W.; Wendt-Potthoff, K. Chemical changes in sediment pore-waters of an acidic mining lake after addition of organic substrate and lime for stimulating lake

remediation. *Water, Air, Soil Pollut.: Focus* **2002**, *2*(3), 123−140.

(30) Nixdorf, B.; Krumbeck, H.; Jander, G.; Beulker, C. Comparison of bacterial and phytoplankton productivity in extremely acidic mining lakes and eutrophic hard water lakes. *Acta Oecol.* **2003**, *24*, 281−288.

(31) Gyure, R. A.; Konopka, A.; Brooks, A.; Doemel, W. Algal and Bacterial Activities in Acidic (pH 3) Strip Mine Lakes. *Appl. Environ. Microbiol.* **1987**, *53*, 2069−2076.

(32) Laskov, C.; Amelung, W.; Peiffer, S. Organic matter preservation in the sediment of an acidic mining lake. *Environ. Sci. Technol.* **2002**, *36*, 4218−4223.

Received for review September 22, 2005. Revised manuscript received February 10, 2006. Accepted February 13, 2006.

ES051874U